Turbulent Gas-Particle Flow in Vertical Risers

Sanjay Dasgupta, Roy Jackson, and Sankaran Sundaresan
Dept. of Chemical Engineering, Princeton University, Princeton, NJ 08544

Many experimental studies on the cross-sectional distribution of particles in vertical risers have revealed marked segregation of particles. These flows are inherently unsteady with large fluctuations in suspension density. In this article, we have analyzed the time-smoothed equations for the motion of dense suspensions to demonstrate the role of these fluctuations on the occurrence of segregation. It is shown that the particles will congregate in regions where the kinetic energy of fluctuations associated with the particles is small. In the context of transport of small particles such as FCC, a simplified model based on the mixture velocity can be constructed. A speculative K-ϵ model based on this velocity is analyzed to illustrate the extent of segregation of particles afforded by unsteady fluctuations.

Introduction

When solid particles are transported by a gas in vertical pipes, experimental studies have shown that they are distributed nonuniformly over the cross section (Bartholomew and Casagrande, 1957; Saxton and Worley, 1970; Yerushalmi et al., 1978; Youchou and Kwauk, 1980; Weinstein et al., 1984; Bader et al., 1988). Consequently, neither quantitative nor qualitative features of the overall behavior can be represented correctly by one-dimensional flow models, which take into account the presence of the pipe walls only through empirically introduced friction factors.

The primary, large-scale mechanical effect of lateral segregation over the cross section is to generate cross-sectional average values of the slip velocity between particles and gas which greatly exceed the local slip anywhere in the pipe. However, the particle concentration profile is also important, because it influences the distribution of residence times of particles, and may even lead to recirculation of particles against the direction of their net flow. These effects are critically important in predicting the behavior of systems in which the particles react chemically with the gas, or catalyze a reaction between substances present in the gas. For example, the riser reactors used for the catalytic cracking of gas oil use a transported solid catalyst, and their performance can be predicted with confidence only if the physical mechanism that determines the cross-sectional distribution of the catalyst can be identified and modeled. Understanding this mechanism is, therefore, of central importance in predicting the behavior of any system in which solid particles are transported through a duct by fluid, and this is the problem addressed here.

Sinclair and Jackson (1989) described a model for fully developed flow in which the interaction of the particles and the gas is restricted to a mutual drag force, whose value depends on the concentration of the particles and the difference between the local average values of the velocities of the gas and particle phases. Since the gas does not slip freely at the wall of the pipe there is a gas velocity profile in fully developed flow, and a corresponding profile of particle velocity is induced by the drag forces exerted by the gas on the particles. As a result of this motion, particles in adjacent layers collide with each other, generating a random component of particle velocity. The kinetic energy of this random motion is analogous to that of the thermal motion of molecules in a gas and, correspondingly, it can be characterized by a "granular temperature" proportional to the mean square of the random component of the particle velocity. The particle velocity fluctuations then generate an effective pressure in the particle phase, together with an effective viscosity which resists shearing of the particle assembly. Both the effective pressure and the effective viscosity depend strongly on the granular temperature, as just defined, so this must be found by solution of a separate differential equation representing a balance for the pseudothermal energy of random motion of the particles. Pseudothermal energy is generated by the working of the effective shear stresses in the particle phase, dissipated by the inelasticity of collisions between particles, and conducted from place to place as a result of gradients in the granular temperature. Thus, a fully developed flow is generated by solving simultaneously three coupled ordinary differential equations, representing force balances for the gas and particle phases, and a conservation equation for the pseudothermal energy of the random component of particle motion.

This model revealed a remarkably rich variety of behavior

over the whole range of possible flow conditions; cocurrent upflow, cocurrent downflow and countercurrent flow. Particle concentration was found to be high near the wall of the duct and, depending on the elastic properties of particle-particle and particle-wall collision, it could also be high near the axis of the tube. Particle recirculation was also observed in situations with a net upflow of particles, and choking and flooding phenomena were indicated.

Pita and Sundaresan (1991) examined the scale-up characteristics predicted by this model and also compared its predictions with experimental data. They demonstrated that the model manifests an unsatisfactory degree of sensitivity to the inelasticity of the particle-particle collisions and the damping of particle-phase fluctuating motion by the gas. It thus follows that it must be missing some key physics. In the absence of any particles, their solution reduces to the Poiseuille solution for fully-developed laminar flow. Recall that, in a laminar flow of a gas, the motion of gas molecules is partitioned into two components, namely, the local mean velocity (of a collection of molecules) and the random fluctuating velocity *at the level of individual molecules*. The motion of the particle phase, as treated by this model, is also laminar, since it recognizes only the local mean velocity and random fluctuations at the level of individual particles. Thus one can label this a *laminar gas-laminar particles* model. It has recently been extended to flow in inclined pipes by Ocone, Sundaresan and Jackson (1993).

High-velocity gas-particle flows in risers are inherently unsteady with large fluctuations in suspension density (Schnitzlein and Weinstein, 1988). The formation of hydrodynamic clusters and streamers has been documented in experiments (Grace and Tuot, 1979; Matsen, 1982; Basu and Nag, 1987; Gidaspow et al., 1989) and in transient simulations of a two-fluid model for gas-particle flows (Tsuo and Gidaspow, 1990). It is then of practical interest to develop a simple hydrodynamic model for the mean (time-smoothed) flow, which retains the essential features that characterize these flows. Such a model will form the basis for analyzing the performance of process units such as riser reactors.

In riser applications, the Reynolds number for the gas flow, based on the diameter of the duct, is high (10^4–10^6) and the flow is, therefore, expected to be turbulent. Louge et al. (1991) have considered the case of large and heavy particles that do not respond to turbulent fluctuations in the gas phase, and constructed a model which is *turbulent gas-laminar particles* in character.

Note that, from the above viewpoint, the origin of turbulence is the inertial instability in the gas phase. In many dense fluid-particle suspensions such as fluidized beds, instabilities leading to phenomena such as bubbling and slugging can be traced to the particle phase inertia. Formation of bubble-like features has been observed in transient integration of volume-averaged equations which neglect the inertial terms in the gas phase, demonstrating that the origin of these instabilities does indeed lie in the particle phase (Hernandez and Jimenez, 1991). In such flows, motion of the particles can be partitioned into three components: the local mean velocity, the fluctuating velocity associated with the organized motion of collections of particle and the fluctuations at the level of individual particles. Mello et al. (1991) and Savage (1992) have shown recently that an inertial instability can come about in a shear flow of a granular material (in the absence of any interstitial gas), giving rise to organized motion of groups of particles. Thus, the presence of an interstitial gas is not always needed to generate instabilities, so it is entirely conceivable that an inertial instability can originate in the collective motion of the particle phase in dense gas-particle flows encountered in risers. A comprehensive physical model should then be *turbulent gas-turbulent particles* in nature, allowing for the generation and dissipation of turbulent kinetic energy in both phases, and exchange of this energy between the phases. (It should be noted that we are calling the organized motion of groups of particles, manifested in the form of persistent fluctuations, particle phase turbulence, simply for lack of a better name. It is not intended to imply that the particle phase fluctuations will exhibit the universal features of turbulent flow of molecular fluids.) Such a model is not available at the present time. Although one can be constructed by formal manipulations of the governing local averaged continuity and momentum balance equations, a large number of speculative closure relations become necessary (Elghobashi and Abou-Arab, 1983; Berker and Tulig, 1986; Ahmadi and Ma, 1990). The application of such models has been limited primarily to very dilute suspensions, where particle-particle collisions, leading to stress transmission through assembly of particles, can be neglected. In gas-particle flows in industrial risers operating in the so-called fast fluidization regime, on the other hand, the particle-particle collisions appear to be very important (Sinclair and Jackson, 1989; Louge et al., 1991).

In this article, we seek to extend the *laminar gas-laminar particles* model of Sinclair and Jackson to a model of the *turbulent gas-turbulent particles* type. Attention will be limited to the case of small particles (for example, FCC catalyst) and high mass loading of solids, typical of common industrial practice, and we shall treat only *the case of fully developed flow* in a vertical pipe. A number of aspects of the model are highly speculative, but the results appear to capture salient features of observations on these systems.

Volume-Averaged Equations of Motion

Volume-averaged continuity and momentum equations for fluid-particle mixtures have been developed by a number of workers, for example, Anderson and Jackson (1967). For flows of gas-particle mixtures and granular materials, where collisions between particles are important, it is now common to invoke the kinetic theory of granular materials and augment the continuity and momentum equations with a balance for the "pseudothermal" energy of particle velocity fluctuations (Johnson and Jackson, 1987; Johnson et al., 1990; Ding and Gidaspow, 1990; Louge et al., 1991). However, in the present preliminary study we will restrict attention to simpler closures for the stress. The volume average equations derived by Anderson and Jackson (1967) are:

$$\phi_g + \phi_s = 1 \tag{1}$$

$$\frac{\partial \phi_g}{\partial t} + \nabla \cdot (\phi_g \underline{u}_g) = 0 \tag{2}$$

$$\frac{\partial \phi_s}{\partial t} + \nabla \cdot (\phi_s \underline{u}_s) = 0 \tag{3}$$

$$\rho_g \frac{\partial}{\partial t}(\phi_g \underline{u}_g) + \rho_g \nabla \cdot (\phi_g \underline{u}_g \underline{u}_g) = \phi_g \nabla \cdot \underline{\underline{E}}_g + \rho_g \phi_g \underline{g} + \beta_1 (\underline{u}_s - \underline{u}_g) \quad (4)$$

$$\rho_s \frac{\partial}{\partial t}(\phi_s \underline{u}_s) + \rho_s \nabla \cdot (\phi_s \underline{u}_s \underline{u}_s) = \nabla \cdot \underline{\underline{E}}_s + \phi_s \nabla \cdot \underline{\underline{E}}_g + \rho_s \phi_s \underline{g} - \beta_1 (\underline{u}_s - \underline{u}_g) \quad (5)$$

Here ϕ_s, ϕ_g and $\underline{u}_s$, $\underline{u}_g$ are the volume fractions and velocities of the two phases, respectively, ρ_s and ρ_g are the densities of the solid material and the gas, $\underline{\underline{E}}_s$ and $\underline{\underline{E}}_g$ are the stress tensors for the two phases, defined in the tensile sense, β_1 is the drag coefficient, and $\underline{g}$ is the specific gravity force. Closures for $\underline{\underline{E}}_s$ and $\underline{\underline{E}}_g$ will be discussed later. A simple expression for β_1, adequate for small particles, is the Richardson-Zaki (1954) equation:

$$\beta_1 = \frac{(\rho_s - \rho_g)\phi_s g}{v_t \phi_g^{n-1}}$$

where v_t is the terminal velocity of fall of an isolated particle under gravity, and the exponent n depends on the Reynolds number, evaluated at this velocity.

The above equations are derived from the point continuity and Navier-Stokes equations for the gas, and Newtonian equations of motion for the individual particles, by local volume averaging, and all variables appearing in them are local averages.

It is important, from the beginning, to distinguish clearly a number of different length scales associated with the systems considered here. The first, and smallest, is the size of a particle. At the volume fractions of interest the separation between neighboring particles is also of this scale. Variations of gas velocity resulting from deformation of the streamlines to pass around and between particles are on the same scale, as are variations in the velocities of individual particles as a result of their interactions with each other by collision, or with fluctuations in the interstitial gas velocity. All phenomena on this scale are erased by the local averaging that leads to Eqs. 1-5 and their physical consequences are subsumed in the closures adopted for the drag coefficient β_1 and the stress tensors $\underline{\underline{E}}_s$ and $\underline{\underline{E}}_g$. These closures may be derived theoretically, as in the use of granular kinetic theory to give an expression for $\underline{\underline{E}}_s$, empirically, as in the use of the Richardson-Zaki equation for β_1, or simply be reasonable guesses, as in the closures we will use here for the stress tensors. The local averaging process then generates a second scale, considerably larger than the particle size and fixed by the size of the averaging volume. Equations 1-5 may be used to describe phenomena down to this scale, but it is meaningless to interpret features of their solutions which are any smaller.

There is, finally, a third scale on which fluctuations in the motion of the two phases may occur, and we assume that this is considerably larger than the scale established by local averaging. The fluctuations in question here arise from phenomena such as the motion of "bubbles" within the suspension or, of particular interest in the present context, phenomena analogous to turbulence in a homogeneous fluid, arising from instabilities of shear flow associated with the presence of solid bounding walls. Such "turbulent" fluctuations correspond to eddies whose sizes range from the pipe diameter down to a characteristic scale analogous to the dissipation length scale in turbulent flow of a homogeneous fluid. It is assumed here that this third scale is considerably larger than the second scale, associated with local averaging. Details of fluctuating motion on the third scale will be erased by time smoothing, as described below, and their physical consequences will be subsumed in the closures used for terms thrown up as correlations by the averaging process; for example, "Reynolds stresses." This is analogous to the procedure used in deriving turbulence models for the mean motion of homogeneous fluids.

Implicit in all these ideas is the assumption that the three length scales described are distinct and well separated, and that the effect on larger-scale phenomena of details of the motion at smaller scales can be conveyed completely by the closures adopted at the smaller scales. To what extent this assumption is justified for the particular system of interest here will be discussed later. For the moment we simply note that, in their study of wave propagation in liquid-fluidized beds, Anderson and Jackson (1969) found that the local averaged equations could correctly capture phenomena at a length scale of about 50 particle diameters. More recent studies of shear flow of a granular material (Mello et al., 1991; Savage, 1992) suggest phenomena on a scale as small as ten particle diameters are captured qualitatively. This establishes an idea of the scale of local averaging.

Dusty Gas Limit

There is a wealth of literature on the influence of suspended particles on turbulent fluid flow. An extensive review is not possible here, but it must be emphasized at the outset that almost all this work is confined to particle concentrations far below the range of interest from the point of view of particle transport systems. Many experiments have been described on vertical pipe flows with suspended spherical particles at mass loadings ranging up to about 6 (see, for example, Soo et al., 1960; Lee and Durst, 1982; Arnason and Stock, 1984; Tsuji et al., 1984). Mass loading is defined as the mass ratio of solids to gas, and values of 50 or higher are typically encountered in applications such as FCC risers. (See Table 1 for typical operating conditions in an FCC Riser Reactor.) At the low mass loadings that have commonly been studied the volume fraction of particles is very small (typically ~ 0.001), so direct particle-particle interactions can be neglected. Equations 1-5 may then be approximated by:

$$\phi_g \approx 1 \quad (6)$$

$$\nabla \cdot (\underline{u}_g) = 0 \quad (7)$$

$$\frac{\partial \phi_s}{\partial t} + \nabla \cdot (\phi_s \underline{u}_s) = 0 \quad (8)$$

$$\rho_g \frac{\partial}{\partial t}(\underline{u}_g) + \rho_g \nabla \cdot (\underline{u}_g \underline{u}_g) = \nabla \cdot \underline{\underline{E}}_g + \rho_g \underline{g} + \tilde{\beta}_1 (\underline{u}_s - \underline{u}_g) \quad (9)$$

$$\rho_s \frac{\partial}{\partial t}(\phi_s \underline{u}_s) + \rho_s \nabla \cdot (\phi_s \underline{u}_s \underline{u}_s) = \rho_s \phi_s \underline{g} - \tilde{\beta}_1 (\underline{u}_s - \underline{u}_g) \quad (10)$$

Table 1. Typical Operating Conditions in an FCC Riser Reactor*

Particle density	1,100–1,500	kg/m^3
Mean particle diameter	50–100	μm
Tube diameter	0.2–2.0	m
Settling velocity	5–20	cm/s
Superficial gas velocity	8–18	m/s
Net solids flux	400–1,400	kg/m$^2\cdot$s
Apparent suspension density	160–650	kg/m^3 at the bottom
	50–80	kg/m^3 at the top

*Adapted from Grace (1990).

where

$$\tilde{\beta}_1 = \frac{(\rho_s - \rho_g)\phi_s g}{v_t} = \alpha\phi_s \quad \text{(say)}.$$

These equations, referred to as the "dusty gas" equations, have been the basis for many theoretical studies (for example, Marble, 1970; Lumley, 1978; Squires and Eaton, 1990). A Newtonian fluid closure is used for $\underline{\underline{E}}_g$ and even the Einstein correction to the viscosity is often discarded (Squires and Eaton, 1990).

Although these equations are quite inadequate to describe the system of interest here, their time-averaged form for fully developed, turbulent pipe flow does indicate, in a fairly simple way, the physical cause of the observed segregation of particles toward the wall. We will, therefore, digress to pursue this point.

Denoting time averages by overbars, Eq. 7 shows that $\nabla\cdot\overline{\underline{u}_g} = 0$ and, for fully developed flow in a pipe of circular section, it follows that $\overline{u}_{gr} = 0$ and $\overline{u}_{gz} = \overline{u}_{gz}(r)$. Also, $\overline{\phi}_s$ is clearly a function of r only, and it is convenient to define a mean velocity $\tilde{\underline{u}}_s$ for the particles by:

$$\overline{\phi}_s\tilde{\underline{u}}_s = \overline{\phi_s\underline{u}_s}$$

Then for the flow considered it follows from Eq. 8 that $\tilde{u}_{sr} = 0$ and $\tilde{u}_{sz} = \tilde{u}_{sz}(r)$.

Defining fluctuations by:

$$\phi_s' = \phi_s - \overline{\phi}_s; \quad \underline{u}_g' = \underline{u}_g - \overline{\underline{u}}_g; \quad \underline{u}_s' = \underline{u}_s - \tilde{\underline{u}}_s$$

the axial and radial components of the time-averaged form of the particle momentum Eq. 10 are:

$$\frac{\rho_s}{r}\frac{d}{dr}\{r[\overline{\phi}_s\overline{(u_{sr}'u_{sz}')} + \overline{(\phi_s'u_{sr}'u_{sz}')}]\} + \rho_s\overline{\phi}_s g + \alpha\overline{\phi}_s(\tilde{u}_{sz} - \overline{u}_{gz}) - \alpha\overline{\phi_s'u_{gz}'} = 0 \quad (11)$$

and

$$\frac{\rho_s}{r}\frac{d}{dr}\{r[\overline{\phi}_s\overline{(u_{sr}'u_{sr}')} + \overline{(\phi_s'u_{sr}'u_{sr}')}]\} - \frac{\rho_s}{r}[\overline{\phi}_s\overline{(u_{s\theta}'u_{s\theta}')} + \overline{(\phi_s'u_{s\theta}'u_{s\theta}')}] - \alpha\overline{(\phi_s'u_{gr}')} = 0 \quad (12)$$

Squires and Eaton (1990) concluded that ϕ_s' is very small in isotropic turbulence provided the Stokes number $\rho_s d_p v_t/\mu_g$ (where μ_g is the gas viscosity) is large. On the basis of this, Rogers and Eaton (1991) argued that the triple correlations in Eqs. 11 and 12 must be small compared to the other Reynolds stress terms and, by the same token, one would expect the contributions from $\overline{(\phi_s'u_{gz}')}$ and $\overline{(\phi_s'u_{gr}')}$ to be small. The equations then reduce to:

$$\frac{\rho_s}{r}\frac{d}{dr}\{r\overline{\phi}_s\overline{(u_{sr}'u_{sz}')}\} + \rho_s\overline{\phi}_s g + \alpha\overline{\phi}_s(\tilde{u}_{sz} - \overline{u}_{gz}) = 0 \quad (13)$$

and

$$\frac{d}{dr}\{r\overline{\phi}_s\overline{(u_{sr}'u_{sr}')}\} - \overline{\phi}_s\overline{(u_{s\theta}'u_{s\theta}')} = 0 \quad (14)$$

These show that fluctuations in particle velocity transfer momentum in the radial direction and, in particular, Eq. 14 shows that the dependence of $\overline{\phi}_s$ on r is closely related to the radial variation of the mean-square velocity fluctuations. This last point is clarified if we make a simplifying assumption that:

$$\overline{(u_{sr}'u_{sr}')} = \overline{(u_{s\theta}'u_{s\theta}')} = \overline{(u_{sz}'u_{sz}')} = \frac{2}{3}K_p \quad \text{(say)}$$

Then Eq. 14 integrates immediately to give:

$$\overline{\phi}_s K_p = \text{constant} \quad (15)$$

Thus, the particle concentration is inversely proportional to the turbulent fluctuation energy per unit mass of particles. Since K_p will necessarily become small close to the pipe wall, $\overline{\phi}_s$ will be large there. Indeed, if one were to demand that $K_p \to 0$ at the wall, as it must, then formally $\overline{\phi}_s \to \infty$ there. However, the dusty gas approximation breaks down long before this (unphysical) limit is approached.

This brief discussion has revealed that the physical origin of the segregation of particles toward the wall is the need to maintain a force balance in the radial direction, despite the variation in the intensity of velocity fluctuations. If the concentration were uniform this would lead to a sharp radial variation in Reynolds stress, and force balance would be impossible.

The above neglects effects such as the Saffman (1965) lift force and Basset forces acting on the particles, though these have been considered in detailed studies of particle deposition at tube walls (see, for example, Rouhiainen and Stachiewics, 1970; Lee and Durst, 1982).

Time-Smoothing of Volume-Averaged Equations of Motion

We now turn attention to the opposite of the dusty gas limit, that is, the case in which the mass loading of particles is high. We shall be particularly interested in particles which are small enough to participate vigorously in velocity fluctuations. Also, their concentration is so large that their interaction, through collisions, is enough to endow the particle phase with a collective behavior of its own. Then, as indicated in the introduction, it is uncertain whether fluctuations in velocity and concentration (which resemble turbulence in a homogeneous fluid) have their origin in an instability of the gas phase, an

instability of the particle phase, or some combination of the two. However, once this type of motion is established, it is certain that the particles are the dominant contributors to both the weight of the suspension and inertial effects. It is, therefore, permissible to simplify the volume averaged Eqs. 1-5 by omitting both inertial and gravitational terms from the gas-phase momentum balance, which then reduces to:

$$\phi_g \nabla \cdot \underline{\underline{E}}_g = \beta_1 (\underline{u}_g - \underline{u}_s) \tag{16}$$

replacing Eq. 4.

We confine attention to fully developed, though not laminar, flow in a vertical pipe. Then the time smoothed values of ϕ_s, ϕ_g, $\underline{u}_s$ and $\underline{u}_g$ are all independent of t and z, as are any correlations of fluctuations in these variables. Thus, the time smoothed form of the gas continuity Eq. 2 reduces to:

$$\frac{1}{r}\frac{\partial}{\partial r}\{r\overline{(\phi_g u_{gr})}\} = 0$$

Integrating and requiring that $\overline{(\phi_g u_{gr})}$ should remain bounded when $r \to 0$ yields $(\phi_g u_{gr}) = 0$, or

$$\bar{\phi}_g \bar{u}_{gr} + \overline{(\phi_g' u_{gr}')} = 0 \tag{17}$$

Similarly the particle phase continuity equation shows that:

$$\bar{\phi}_s \bar{u}_{sr} + \overline{(\phi_s' u_{sr}')} = 0 \tag{18}$$

Physically, $\overline{(\phi_g' u_{gr}')}$ and $\overline{(\phi_s' u_{sr}')}$ represent radial transport of gas or particles, respectively, by correlated fluctuations in concentration and velocity; in other words, "turbulent dispersion." Then Eqs. 17 and 18 lead us to anticipate that $\bar{u}_{gr}$ and $\bar{u}_{sr}$ will be small in comparison with the time smoothed axial components of velocity, or any components of the velocity fluctuations. This observation will be important later.

Again, invoking the fully developed nature of the flow, the time smoothed form of the axial component of the particle phase momentum Eq. 5 is:

$$\frac{\rho_s}{r}\frac{\partial}{\partial r}\{r[\bar{\phi}_s \bar{u}_{sr}\bar{u}_{sz} + \bar{\phi}_s\overline{(u_{sr}'u_{sz}')} + \bar{u}_{sr}\overline{(\phi_s' u_{sz}')} + \bar{u}_{sz}\overline{(\phi_s' u_{sr}')}]\}$$
$$= \overline{(\nabla \cdot \underline{\underline{E}}_s)_z} + \overline{(\phi_s \nabla \cdot \underline{\underline{E}}_g)_z} - \rho_s \bar{\phi}_s g + \overline{\beta_1 (u_{gz} - u_{sz})}$$

where the third-order correlation $\overline{(\phi_s' u_{sr}' u_{sz}')}$ has been neglected. But from Eq. 18 the first and last terms cancel in the square brackets on the lefthand side. Also, since $\overline{(\phi_s' u_{sz}')}$ represents axial turbulent dispersion, we expect it to be proportional to $(\partial \bar{\phi}_s / \partial z)$, which vanishes for fully developed flow. Thus, the equation reduces to:

$$\frac{\rho_s}{r}\frac{\partial}{\partial r}\{r[\bar{\phi}_s\overline{(u_{sr}'u_{sz}')}]\} = \overline{(\nabla \cdot \underline{\underline{E}}_s)_z} + \overline{(\phi_s \nabla \cdot \underline{\underline{E}}_g)_z}$$
$$- \rho_s \bar{\phi}_s g + \overline{\beta_1 (u_{gz} - u_{sz})} \tag{19}$$

The time smoothed form of the axial component of the gas-phase momentum balance (Eq. 16) is:

$$\overline{(\phi_g \nabla \cdot \underline{\underline{E}}_g)_z} - \overline{\beta_1 (u_{gz} - u_{sz})} = 0$$

and adding this to Eq. 19 gives:

$$\frac{\rho_s}{r}\frac{\partial}{\partial r}\{r\bar{\phi}_s\overline{(u_{sr}'u_{sz}')}\} = \overline{(\nabla \cdot \underline{\underline{E}})_z} - \rho_s \bar{\phi}_s g \tag{20}$$

where

$$\underline{\underline{E}} = \underline{\underline{E}}_s + \underline{\underline{E}}_g$$

Equation 20 may be regarded as a time smoothed axial momentum balance for the suspension.

The radial components of momentum balance for both phases may be time-smoothed in the same way and, after adding the resulting expressions, the following radial, time smoothed momentum balance for the suspension is obtained:

$$\frac{\rho_s}{r}\frac{\partial}{\partial r}\{r[\bar{\phi}_s\overline{(u_{sr}'u_{sr}')} + \bar{u}_{sr}\overline{(\phi_s' u_{sr}')}]\}$$
$$- \frac{\rho_s}{r}\bar{\phi}_s\overline{(u_{s\theta}'u_{s\theta}')} = \overline{(\nabla \cdot \underline{\underline{E}})_r} \tag{21}$$

Note the appearance in this equation of the correlation $\overline{(\phi_s' u_{sr}')}$, representing dispersion in the radial direction. A corresponding term $\overline{(\phi_s' u_{sz}')}$ was eliminated from the axial momentum balance by noting that it should be proportional to the (vanishing) gradient $\partial \bar{\phi}_s / \partial z$. Similarly, $\overline{(\phi_s' u_{sr}')}$ should be proportional to $\partial \bar{\phi}_s / \partial r$ but this does not vanish. However, using Eq. 18, we can write:

$$\bar{u}_{sr}\overline{(\phi_s' u_{sr}')} = -\bar{\phi}_s \bar{u}_{sr}\bar{u}_{sr}$$

As noted earlier, we expect $|\bar{u}_{sr}|$ to be much smaller than $|u_{sr}'|$, so that $|\bar{\phi}_s \bar{u}_{sr}\bar{u}_{sr}| \ll |\bar{\phi}_s\overline{(u_{sr}'u_{sr}')}|$, and the second term in square brackets on the lefthand side of Eq. 21 is much smaller than the first. We would therefore be justified in dropping this term immediately but, since it can be retained without causing difficulty later, we will defer this judgment.

We must now make more precise our statement that we confine attention to "small" particles. Our argument that inertial effects associated with the particle phase dominate those associated with the gas phase depends, not only on the mass concentration of particles dominating that of gas, but also on all relevant components of particle velocity being comparable in magnitude with the corresponding components of gas velocity. The magnitude of the slip velocity $\underline{u}_g - \underline{u}_s$ depends on the drag coefficient β_1 and, if β_1 is large, $|\underline{u}_g - \underline{u}_s|$ is small of order $1/\beta_1$. But β_1 increases as the particle size decreases, and we require the particles to be so small that the slip velocity is everywhere small in magnitude compared with $\bar{u}_{sz}$, u_{sz}', u_{sr}' and $u_{s\theta}'$. Since we are concerned with a high solids loading at which the "turbulent" fluctuations are driven by the collective motion of the particle assembly, rather than the gas, the slip velocity will be small, in the above sense, only if the relaxation time for the gas velocity to conform to that of the particles is short compared with the shortest significant time scale of the fluctuations in particle velocity. If the slip is small, in this sense, it is not necessary to distinguish between solids and gas for the above velocity components, and henceforth we will, therefore, drop the suffix "s" on them. However, it is important to recognize that this argument does not justify ne-

glecting the difference between $\bar{u}_{gr}$ and $\bar{u}_{sr}$, since these are much smaller than the other velocity components and may be comparable in magnitude with the slip.

Introducing the components of $\underline{\underline{E}}$ explicitly and erasing the suffix s from the velocity components, Eqs. 20 and 21 become:

$$\frac{1}{r}\frac{\partial}{\partial r}\{r\overline{\rho(u_r'u_z')}\}=\frac{1}{r}\frac{\partial}{\partial r}\{r\bar{E}_{rz}\}+\frac{\partial\bar{E}_{zz}}{\partial z}-\bar{\rho}g \tag{22}$$

and

$$\frac{1}{r}\frac{\partial}{\partial r}\{r[\overline{\rho(u_r'u_r')}+\bar{u}_{sr}\overline{(\rho'u_r')}]\}-\frac{\bar{\rho}}{r}\overline{(u_\theta'u_\theta')}$$
$$=\frac{1}{r}\frac{\partial}{\partial r}\{r\bar{E}_{rr}\}-\frac{\bar{E}_{\theta\theta}}{r}+\frac{\partial\bar{E}_{rz}}{\partial z} \tag{23}$$

where $\bar{\rho}=\rho_s\bar{\phi}_s$ is the time smoothed bulk density of the suspension.

To make these equations explicit a closure relation is needed for $\underline{\underline{\bar{E}}}$, and later we will also need one for $\underline{\underline{\bar{E}}}_g$. It has been common practice to adopt the Newtonian fluid form of closure for the volume averaged tensors $\underline{\underline{E}}_s$ and $\underline{\underline{E}}_g$ in the starting Eqs. 4 and 5, with effective viscosities and the pressure term in $\underline{\underline{E}}_s$ specified as explicit functions of the suspension density ρ. Time averaging then generates more complicated expressions for the time smoothed tensors $\underline{\underline{\bar{E}}}_s$ and $\underline{\underline{\bar{E}}}_g$, because of correlations involving fluctuations of ρ. Since the Newtonian fluid form for $\underline{\underline{E}}_s$ and $\underline{\underline{E}}_g$ is, itself, without a firm physical basis, we shall bypass this procedure altogether and simply assume Newtonian closures directly for the time smoothed tensors:

$$\underline{\underline{\bar{E}}}=-\bar{p}(\bar{\rho})\underline{\underline{I}}+\mu_e(\bar{\rho})[\underline{\underline{\nabla\bar{u}}}+(\underline{\underline{\nabla\bar{u}}})^T] \tag{24}$$

and

$$\underline{\underline{\bar{E}}}_g=-\bar{p}_g\underline{\underline{I}}+\mu_{eg}(\bar{\rho})[\underline{\underline{\nabla\bar{u}}}+(\underline{\underline{\nabla\bar{u}}})^T] \tag{25}$$

with $\bar{p}(\bar{\rho})=\bar{p}_g+\bar{p}_s(\bar{\rho})$ and $\bar{p}_s$, the effective pressure exerted by collisions between particles, assumed to depend only on particle concentration (which determines $\bar{\rho}$). The explicit functional forms chosen for $\bar{p}_s(\bar{\rho})$, $\mu_e(\bar{\rho})$ and $\mu_{eg}(\bar{\rho})$ will be specified later.

Using Eq. 24 we find that:

$$\bar{E}_{rr}=\bar{E}_{\theta\theta}=\bar{E}_{zz}=-\bar{p};\quad \bar{E}_{rz}=\mu_e\frac{\partial\bar{u}_z}{\partial r}$$

for fully developed flow. Also $\partial\bar{p}_s/\partial z=0$, since $\bar{\rho}$ is independent of z, so $\partial\bar{p}/\partial z=\partial\bar{p}_g/\partial z$. With these results Eqs. 22 and 23 become:

$$\frac{1}{r}\frac{\partial}{\partial r}\left\{r\left[\mu_e\frac{\partial\bar{u}_z}{\partial r}-\bar{\rho}\overline{(u_r'u_z')}\right]\right\}=\bar{\rho}g+\frac{\partial\bar{p}_g}{\partial z} \tag{26}$$

and

$$\frac{1}{r}\frac{\partial}{\partial r}\{r[\overline{\rho(u_r'u_r')}+\bar{u}_{sr}\overline{(\rho'u_r')}]\}-\frac{\overline{\rho(u_\theta'u_\theta')}}{r}+\frac{\partial\bar{p}_s}{\partial r}=-\frac{\partial\bar{p}_g}{\partial r} \tag{27}$$

It now remains to evaluate the term $\partial\bar{p}_g/\partial r$, and for this purpose we divide the radial component of Eq. 16 by ϕ_g, then time smooth, giving:

$$-\frac{\partial\bar{p}_g}{\partial r}=\overline{\beta(\phi_s)(u_{gr}-u_{sr})} \tag{28}$$

where $\beta=\beta_1/\phi_g$. As noted above, the difference between u_{gr} and u_{sr} is not necessarily small compared with these quantities individually and, furthermore, it is multiplied by the large factor β. However, if we use the approximation,

$$\beta(\phi_s)\approx\beta(\bar{\phi}_s)+\left(\frac{d\beta}{d\phi_s}\right)_{\bar{\phi}_s}\phi_s'$$

Equation 28 may be expanded as:

$$-\frac{\partial\bar{p}_g}{\partial r}=\beta(\bar{\phi}_s)(\bar{u}_{gr}-\bar{u}_{sr})+\left(\frac{d\beta}{d\phi_s}\right)_{\bar{\phi}_s}\overline{\phi_s'(u_{gr}'-u_{sr}')}$$

or, introducing expressions for $\bar{u}_{gr}$ and $\bar{u}_{sr}$ found from Eqs. 17 and 18:

$$-\frac{\partial\bar{p}_g}{\partial r}=\beta(\bar{\phi}_s)\left(\frac{\overline{(\phi_s'u_{sr}')}}{\bar{\phi}_s}-\frac{\overline{(\phi_g'u_{gr}')}}{\bar{\phi}_g}\right)$$
$$+\left(\frac{d\beta}{d\phi_s}\right)_{\phi_s}(\overline{(\phi_s'u_{gr}')}-\overline{(\phi_s'u_{sr}')})$$

Since $\phi_g=1-\phi_s$ this can also be written:

$$-\frac{\partial\bar{p}_g}{\partial r}=\beta(\bar{\phi}_s)\left(\frac{\overline{(\phi_s'u_{sr}')}}{\bar{\phi}_s}+\frac{\overline{(\phi_s'u_{gr}')}}{1-\bar{\phi}_s}\right)$$
$$+\left(\frac{d\beta}{d\phi_s}\right)_{\phi_s}[\overline{(\phi_s'u_{gr}')}-\overline{(\phi_s'u_{sr}')}]$$

then, setting $u_{sr}'=u_{gr}'=u_r'$ on the righthand side:

$$-\frac{\partial\bar{p}_g}{\partial r}=\frac{\beta(\bar{\phi}_s)}{\bar{\phi}_s(1-\bar{\phi}_s)}\overline{(\phi_s'u_r')}=\frac{\beta(\bar{\rho})\rho_s}{\bar{\rho}(\rho_s-\bar{\rho})}\overline{(\rho'u_r')} \tag{29}$$

Using this, in Eq. 27 and eliminating $\bar{u}_{sr}$ from the lefthand side of that equation using Eq. 18, we then find:

$$\frac{1}{r}\frac{\partial}{\partial r}\left\{r\left[\overline{\rho(u_r'u_r')}-\frac{\overline{(\rho'u_r')^2}}{\bar{\rho}}\right]\right\}-\bar{\rho}\frac{\overline{(u_\theta'u_\theta')}}{r}$$
$$+\frac{\partial\bar{p}_s}{\partial r}=\frac{\rho_s\beta(\bar{\rho})}{\bar{\rho}(\rho_s-\bar{\rho})}\overline{(\rho'u_r')} \tag{30}$$

Equations 26 and 30 are our time smoothed axial and radial momentum balances for the suspension.

Turbulence Model

Subject to our assumptions of high mass loading and small particles, Eqs. 26 and 30 are formal consequences of time smoothing, and are appropriate whatever the physical phenomena responsible for the fluctuations in the variables. For

example, these could be consequences of "bubbles" of low particle concentration rising within the suspension, a phenomenon very familiar in dense gaseous suspensions of solid particles. At the high flow rates of greatest technical interest, on the other hand, it is reasonable to suppose that the fluctuations result from an instability of the shear flow associated with the presence of a solid bounding wall; in other words, they are analogous to turbulent fluctuations in a homogeneous fluid. In that case, we may speculate that the equations can be closed by a turbulence model, for example, a simple model of the well-known K-ϵ type. If so, we neglect the anisotropy of the velocity fluctuations and write:

$$\overline{(u_r'u_r')} = \overline{(u_\theta'u_\theta')} = \frac{2}{3}K \tag{31}$$

We also introduce a turbulent kinematic viscosity ν_T and write:

$$\overline{(u_r'u_z')} = -\nu_T \frac{\partial \bar{u}_z}{\partial r} \tag{32}$$

and it is reasonable to expect the turbulent dispersion flux to be given by:

$$\overline{(\rho' u_r')} = -\nu_T \frac{\partial \bar{\rho}}{\partial r} \tag{33}$$

Equations 26 and 30 then become:

$$\frac{1}{r}\frac{\partial}{\partial r}\left\{r\left[(\mu_e + \bar{\rho}\nu_T)\frac{\partial \bar{u}_z}{\partial r}\right]\right\} = \bar{\rho}g + \frac{\partial \bar{p}_g}{\partial z} \tag{34}$$

and

$$\frac{\partial}{\partial r}\left(\frac{2}{3}\bar{\rho}K + \bar{p}_s\right) - \frac{1}{r}\frac{\partial}{\partial r}\left\{\frac{r\nu_T^2}{\bar{\rho}}\left(\frac{\partial \bar{\rho}}{\partial r}\right)^2\right\} + \frac{\rho_s \beta(\bar{\rho})}{\bar{\rho}(\rho_s - \bar{\rho})}\nu_T \frac{\partial \bar{\rho}}{\partial r} = 0 \tag{35}$$

It now remains only to determine K and ν_T, and we speculate that a closure of the K-ϵ type, which has had some success in turbulent single-phase flows, might be appropriate. When the density of the material is variable, as is the case here, a number of correlations appear in the balance equations for K and ϵ which are not present in the case of an incompressible fluid (Cebeci and Smith, 1974). As a tentative first attempt at closure, we will explore the consequences of simply neglecting these terms and using the well-known K-ϵ equations for a fluid of constant density (Speziale, 1991), namely,

$$\nu_T = \frac{C_\mu K^2}{\epsilon} \tag{36}$$

$$\frac{1}{r}\frac{\partial}{\partial r}\left\{r\left(\frac{\bar{\rho}\nu_T}{\sigma_K} + \mu_e\right)\frac{\partial K}{\partial r}\right\} + \bar{\rho}\nu_T\left(\frac{\partial \bar{u}_z}{\partial r}\right)^2 - \bar{\rho}\epsilon = 0 \tag{37}$$

$$\frac{1}{r}\frac{\partial}{\partial r}\left\{r\left(\frac{\bar{\rho}\nu_T}{\sigma_\epsilon} + \mu_e\right)\frac{\partial \epsilon}{\partial r}\right\} + C_{\epsilon 1}\frac{\epsilon}{K}\bar{\rho}\nu_T\left(\frac{\partial \bar{u}_z}{\partial r}\right)^2 - C_{\epsilon 2}\frac{\epsilon^2}{K}\bar{\rho} = 0 \tag{38}$$

where σ_K, σ_ϵ, $C_{\epsilon 1}$ and C_μ are empirically assigned constants, whose values in Table 2 are typical of those used for a homogeneous, incompressible fluid. The standard K-ϵ model, with $C_{\epsilon 2}$ also constant, cannot be integrated up to the pipe wall. Either the solution must be matched to functions representing the behavior of K and ϵ near the wall, or some form of damping must be introduced (Patel et al., 1985). However, a model which is formally integrable up to the wall can be obtained if $C_{\epsilon 2}$ is allowed to vary with radial position so that it tends to zero in a particular way on approaching the wall (Patel et al., 1985). Specifically,

$$C_{\epsilon 2} = C_2[1 - \exp(-R_T^2)] \tag{39}$$

where $R_T = K^2/\nu_e\epsilon$, with $\nu_e = \mu_e/\bar{\rho}$, and C_2 is a constant whose assumed value is listed in Table 2.

Table 2. Parameters of Turbulence Model

Particle density,	$\rho_s = 1{,}500$ kg/m^3
Particle diameter,	$d_p = 100$ μm
Terminal velocity,	$v_t = 0.2$ m/s
Solids volume fraction at random close packing,	$\phi_{sm} = 0.65$
Richardson-Zaki exponent,	$n = 3.5$
Gas viscosity,	$\mu_g = 4 \times 10^{-5}$ kg/m·s
Tube radius,	$R = 0.15$ m
Solid-phase effective pressure factor,	$A = 20$ N/m^2
Solid-phase effective viscosity factor,	$B = 0.09$ kg/m·s
K-ϵ Model Parameters	
$C_{\epsilon 1} = 1.45$; $C_2 = 2.0$; $\sigma_\epsilon = 1.3$; $\sigma_K = 1.0$; $C_\mu = 0.09$	

The particle phase effective pressure $\bar{p}_s$ and viscosity μ_{es} are assumed to be given by:

$$\bar{p}_s = A\bar{\phi}_s(1 + 4\bar{\phi}_s g_o) \tag{40}$$

and

$$\mu_{es} = B\left[\frac{(1 + 1.6\,\bar{\phi}_s g_o)^2}{g_o} + 9.779\,\bar{\phi}_s^2 g_o\right] \tag{41}$$

where $g_o = 1/[1 - (\bar{\phi}_s/\phi_{sm})^{1/3}]$ and ϕ_{sm} is the value of ϕ_s at random close packing. These are consistent in form with the predictions of granular kinetic theory (see, for example, Lun et al., 1984), but kinetic theory also relates the factors A and B to granular temperature. Since we do not calculate granular temperature, A and B are simply assigned numerical values, which are listed in Table 2. Work is in progress on a treatment including the pseudothermal energy balance, which will eliminate these adjustable parameters.

The form assumed for the effective viscosity of the gas phase is:

$$\mu_{eg} = \mu_g(1 + 2.5\,\bar{\phi}_s + 7.6\,\bar{\phi}_s^2)(1 - \bar{\phi}_s/\phi_{sm}) \tag{42}$$

the same as that employed by Sinclair and Jackson (1989). The effective viscosity of the suspension, μ_e, is simply equal to $\mu_{es} + \mu_{eg}$.

Finally, since the model takes the form of coupled differential equations for $\bar{u}_z$, $\bar{\rho}$, K and ϵ, boundary conditions are needed at the pipe wall. When interactions between the particles and the wall are due to collisions, boundary conditions for $\bar{u}_z$

have been derived by a number of workers. In particular, for particles as small as FCC, Pita and Sundaresan (1991) pointed out that the boundary condition used by Johnson and Jackson (1987) approximates closely the no-slip condition $\bar{u}_z = 0$. We shall, therefore, demand that $\bar{u}_z$ should vanish at the wall. Clearly K must also vanish at the wall, and for ϵ at the wall we note, following Patel et al. (1985), that:

$$\epsilon = 2\nu_e \left(\frac{\partial K^{1/2}}{\partial r} \right)^2$$

where $\nu_e = \mu_e / \bar{\rho}$. The choice of the value of $\bar{\rho}$ at the wall is available to determine the average particle loading in the suspension.

This completes the model, but for practical purposes we need the volume flow rate, or superficial velocity of each phase. For the solid phase this is given by:

$$\bar{U}_s = \frac{Q_s}{\pi R^2} = \frac{2}{R^2} \int_o^R \overline{r(\phi_s u_z)} dr$$

where R is the pipe radius and Q_s the total volume flow of solid material. This may be expanded as:

$$\bar{U}_s = \frac{2}{R^2} \int_o^R r[\bar{\phi}_s \bar{u}_z + \overline{(\phi_s' u_z')}] dr$$

The second term represents axial turbulent dispersion and vanishes for fully developed flow, as noted earlier, so this reduces to:

$$\bar{U}_s = \frac{2}{R^2} \int_o^R r \bar{\phi}_s \bar{u}_z dr$$

and similarly

$$\bar{U}_g = \frac{2}{R^2} \int_o^R r(1 - \bar{\phi}_s) \bar{u}_z dr.$$

Results and Discussion

The two point boundary value problem, defined by the momentum Eqs. 34 and 35 and the K-ϵ Eqs. 37 and 38, together with their boundary conditions, was solved using a Galerkin method with 13 elements spanning the radius of the tube. Within each element, integrals were evaluated using a four point quadrature. The results were checked both by increasing the number of elements and changing their radial distribution and, provided enough elements were placed near the wall to resolve the rather rapid variations there, the computed profiles were not changed significantly. Increasing the number of quadrature points from four to six also had a negligible effect on the results. We are, therefore, confident that the computed profiles correctly represent solutions of the equations.

Figures 1-4 show the computed radial profiles of velocity $\bar{u}_z$, solids volume fraction $\bar{\phi}_s$, turbulent fluctuation energy K, and rate of dissipation of turbulent fluctuations per unit volume, $\bar{\rho}\epsilon$. These correspond to the values listed in Table 2 for the physical parameters and the constants in the model. The superficial gas velocity is 5 m/s, the solids flux is 100 kg/m^2·s,

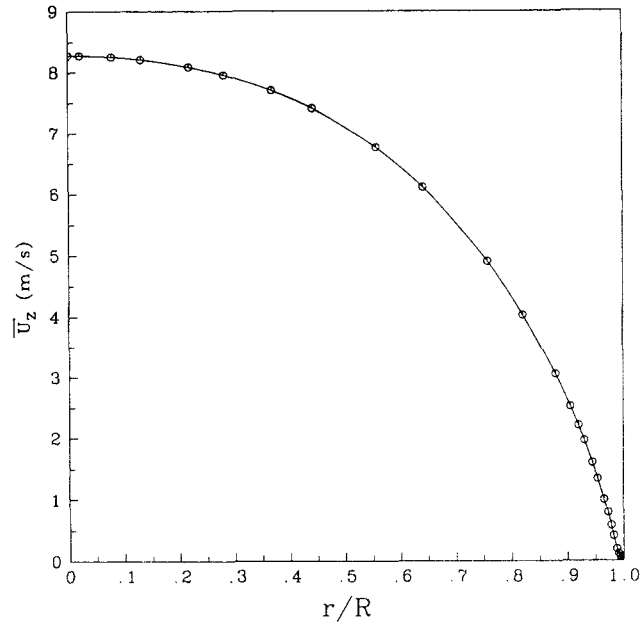

Figure 1. Radial variation of $\bar{u}_z$.
$\bar{U}_s = 0.067$ m/s and $\bar{U}_g = 5$ m/s. See Table 2 for values of all other parameters.

and the computed value for the axial gradient of gas pressure is 598 N/m^3. The particle properties, the fluxes of gas and solids, and the diameter of the pipe were chosen to be close to ranges of commercial interest. The values of the parameters in the K-ϵ model are typical of those used to model turbulent flow of a homogeneous fluid. Though the computations were carried out in terms of suitably scaled dimensionless variables, we have chosen to present the result in terms of dimensional quantities to facilitate comparison with commercial operating experience.

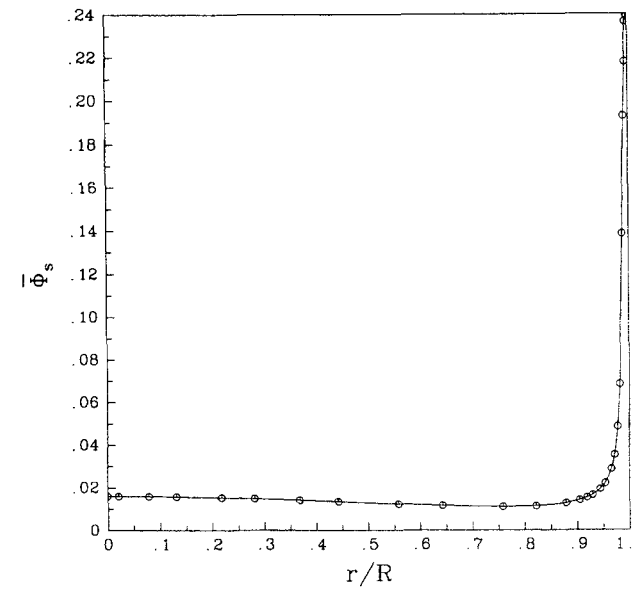

Figure 2. Radial variation of $\bar{\phi}_s$.
$\bar{U}_s = 0.067$ m/s and $\bar{U}_g = 5$ m/s. See Table 2 for values of all other parameters.

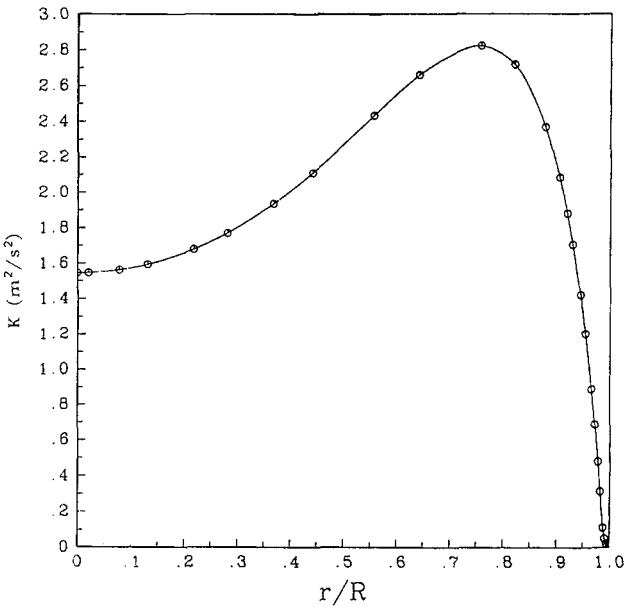

Figure 3. Radial variation of K.

$\overline{U}_s = 0.067$ m/s and $\overline{U}_g = 5$ m/s. See Table 2 for values of all other parameters.

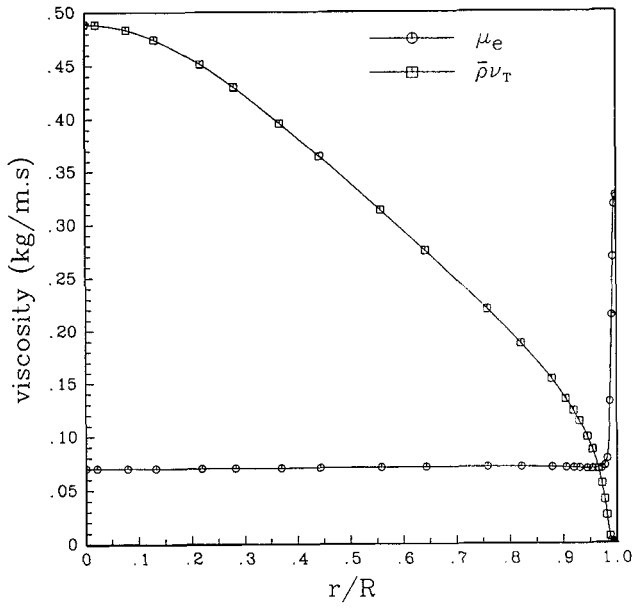

Figure 5. Radial variation of turbulent viscosity ($\overline{\rho}\nu_T$) and laminar mixture viscosity (μ_e).

Note, first, that the profile of solids volume fraction (Figure 2) shows very clearly the strong segregation of particles toward the pipe wall. The suspension contains about 1.5% by volume of solids from the axis to approximately $r = 0.9\ R$, but for larger values of r this rises rapidly, reaching almost 25% by volume at the wall. The particle concentration is actually smallest near $r = 0.8\ R$, with a slight increase from there toward the center of the pipe. This reflects the dip in the K profile in the center of the pipe, seen in Figure 3, together with the dominance of the first term in the radial force balance (Eq. 35).

The shape of the velocity profile (Figure 1) reflects the influence of the distribution of particle concentration. Compared with the turbulent velocity profile for a homogeneous fluid it is less flat; indeed, it looks more like the parabolic profile of laminar flow. This reflects the fact that the resistance to gas flow is lower on the axis of the pipe than near the wall, so there is a tendency for the gas flow to concentrate near the axis.

The K-profile (Figure 3) resembles (qualitatively) that for a homogeneous fluid. Though the behavior as $r/R \to 1$ cannot be seen easily on the scale of the diagram, an enlargement of this region shows clearly that both K and $\partial K/\partial r$ tend to zero when $r/R \to 1$, as expected. The small values of K near the wall are consistent with the high values of $\overline{\rho}\epsilon$ there, as shown in Figure 4.

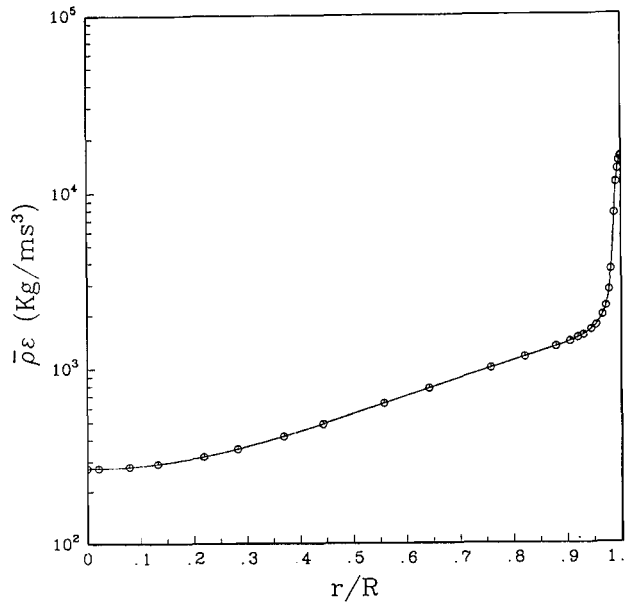

Figure 4. Radial variation of $\overline{\rho}\epsilon$.

$\overline{U}_s = 0.067$ m/s and $\overline{U}_g = 5$ m/s. See Table 2 for values of all other parameters.

Figures 5 and 6 compare the values of various terms appearing in the axial and radial momentum balances, Eqs. 34 and 35. Figure 5 shows the "laminar" and "turbulent" contributions to viscosity, μ_e and $\overline{\rho}\nu_T$, respectively, and these behave in the expected way. μ_e remains constant at about 0.7 poise over most of the cross section but rises steeply in the thin layer of high particle concentration near the wall, reaching a value of 3.3 poise at the wall, where the particle concentration is about 25% by volume. These figures are of the order to be expected from measurements of viscosity of gaseous suspensions. μ_e is, of course, totally dominated by μ_{es}, and μ_{eg} could be replaced by zero, without significantly changing the results. The "turbulent" contribution to viscosity arising from the Reynolds stress, increases from zero at the wall to a maximum value of almost 5 poise on the axis.

Figure 6 shows the terms $2/3\ \overline{\rho}\ K$ and $\overline{p}_s$ appearing on the lefthand side of Eq. 35. As expected, $\overline{p}_s$ is small over most of the cross section, increasing rapidly in the layer of high concentration near the wall, while $2/3\ \overline{\rho}\ K$ is zero at the wall and increases on moving toward the axis. The dip in the value of this variable in the center of the pipe reflects the corresponding dip in K (see Figure 3), of course.

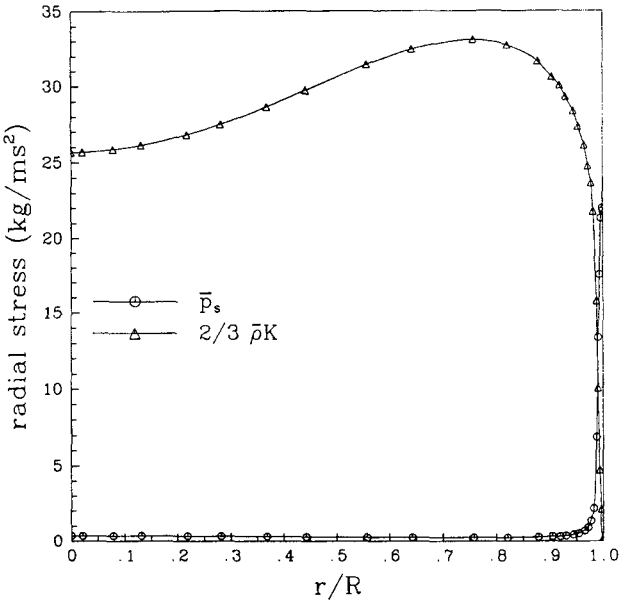

Figure 6. Radial variation of terms in the radial momentum balance: particle pressure ($\bar{p}_s$) and Reynolds stress [(2/3)$\bar{\rho}K$].

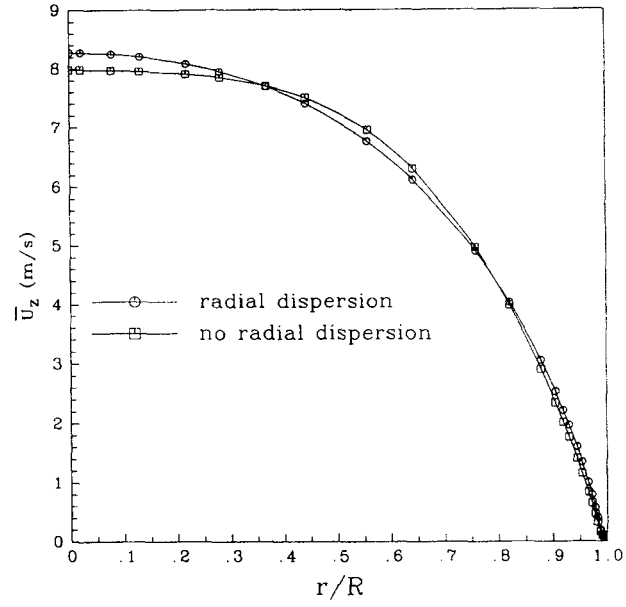

Figure 8. Mean axial velocity profiles with and without radial dispersion.

The two remaining terms in Eq. 35 depend on the radial dispersion velocity ($\overline{\phi_s' u_r'}$), which is given by $\nu_T \partial \bar{\phi}_s / \partial r$ according to Eq. 33. In developing the equations of the model we assumed that this was small compared with $\bar{u}_z$ and the fluctuations in velocity components. Figure 7 shows ($\overline{\phi_s' u_r'}$) as a function of r, and it is seen that its magnitude nowhere exceeds 0.01 m/s. From Figure 1, on the other hand, $\bar{u}_z$ rises to between 8 and 9 m/s at the axis, and its mean value over the cross section is almost half that. Even where ($\overline{\phi_s' u_r'}$) takes its largest value (0.01 m/s at $r/R \approx 0.97$), the value of $\bar{u}_z$ is approximately 0.5 m/s, so it is certainly justified to neglect the dispersion velocity compared with $\bar{u}_z$. According to Eq. 31, the magnitudes of the fluctuating components of velocity are of the order of $(2/3\,K)^{1/2}$ and from Figure 3 we again see that this is much larger than ($\overline{\phi_s' u_r'}$), even where this takes it largest value, so it is also justified to neglect the dispersion velocity compared with the velocity fluctuations. The same comparison shows that contributions from the term in braces on the lefthand side of Eq. 35 are negligible compared with contributions from the term $2/3\,\bar{\rho}\,K$ so, as we anticipated, the equations could be simplified by dropping this term without any significant consequences.

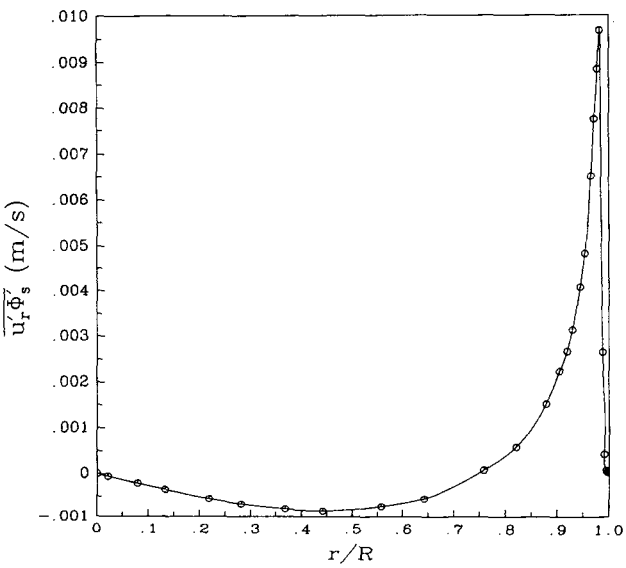

Figure 7. Radial variation of radial dispersion velocity.

It is not so easy to dismiss the last term in Eq. 35, which represents the mechanical effect of the radial dispersion flux, since in this term the small dispersion velocity is multiplied by the large drag coefficient β. Consequently, we repeated the computations, in their entirety, with this term deleted from Eq. 35. Figures 8 and 9 then compare the velocity and solids fraction profiles obtained with, and without this term. The radial dispersion term is seen to flatten the solids fraction profile somewhat in the central part of the pipe, and to spread the dense layer at the wall a little wider. These are exactly the effects to be expected, but they are small, so we can conclude that turbulent dispersion plays a rather minor role in determining the distribution of particle concentration; its influence is secondary to that of the Reynolds stress.

Having found a solution, it is important to retrace our steps and check retrospectively whether the assumptions about relative sizes of different length and time scales, on which our equations were founded, are indeed satisfied for this solution.

First consider length scales. It is reasonable to use the volume-averaged equations of motion only if the particle size, and the mean spacing between adjacent particles, are small compared with the dissipation length scale of the turbulent eddies. The order of magnitude of the spacing, λ, as a function of the volume fraction of solids, can be estimated by imagining the particles to be placed on the points of a regular, cubic lattice. The dissipation scale, on the other hand, is given by:

$$l_K = (\nu_e^3/\epsilon)^{1/4}$$

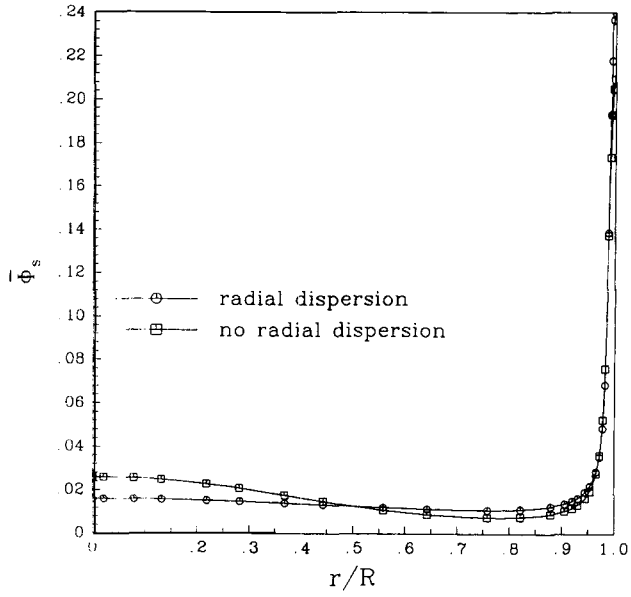

Figure 9. Mean solids volume fraction profiles with and without radial dispersion.

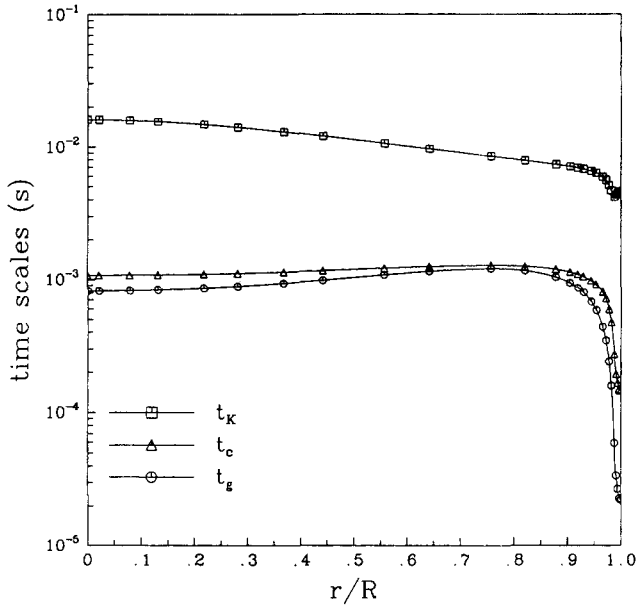

Figure 11. Radial variation of time scales associated with the flow: dissipation time (t_K), collision time (t_c) and gas relaxation time (t_g).

Then from Figure 10, which shows both these length scales as multiples of the particle diameter, it is seen that the particle separation is of the same order as the particle size, or smaller, everywhere in the cross section. The dissipation scale, on the other hand, is about thirty times larger, so our assumption about the ordering of these scales was justified.

The important time scales are the mean time t_c between collisions of a particle with its neighbors, the relaxation time t_g for the gas velocity to approach the particle velocity, and the dissipation time scale t_K for the turbulent eddies. t_c is given by λ/c, where c is the mean velocity of pseudothermal motion of a particle, generated by its collisions with its neighbors. c can be estimated by comparing the parameter A, appearing in the expression (Eq. 40) for $\bar{p}_s$, with the expression for this factor predicted from granular kinetic theory by Lun et al. (1984). The latter relates A to the granular temperature T, which is in turn linked to c by $T = 1/3\ c^2$. In this way, we find:

$$c = \sqrt{\frac{3A}{\rho_s}}$$

Using the value of A from Table 2 and values of λ from Figure 10 this gives the curve of t_c shown in Figure 11.

The gas relaxation time t_g is found from the gas momentum Eq. 4, specialized to the case of one-dimensional flow through an assembly of particles at rest, with zero gravity force. Then, using Eq. 2, Eq. 4 reduces to:

$$\rho_g \phi_g \frac{Du_g}{Dt} = -\beta_1 u_g$$

It follows immediately that the relaxation time is given by:

$$t_g = \frac{\rho_g \phi_g}{\beta_1} = \frac{\rho_g}{\beta} = \frac{\rho_g v_t \bar{\phi}_g^n}{(\rho_s - \rho_g)\bar{\phi}_s g}$$

where the Richardson-Zaki expression has been inserted for β. The motion of the particles in the gas is Stokesian, even at their terminal velocity of fall, where the Reynolds number based on particle diameter is approximately 0.6, so we can write:

$$v_t = \frac{1}{18} \frac{d^2 \rho_s g}{\mu_g}$$

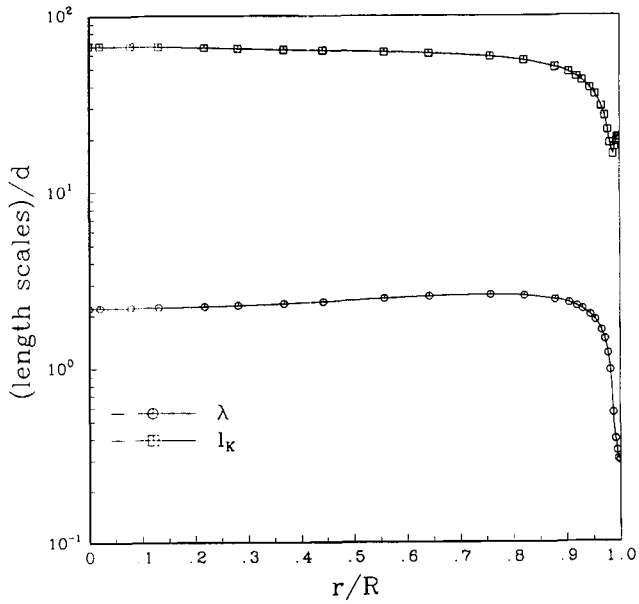

Figure 10. Radial variation of length scales associated with the flow: mean separation between particles (λ) and dissipation scale (l_K).

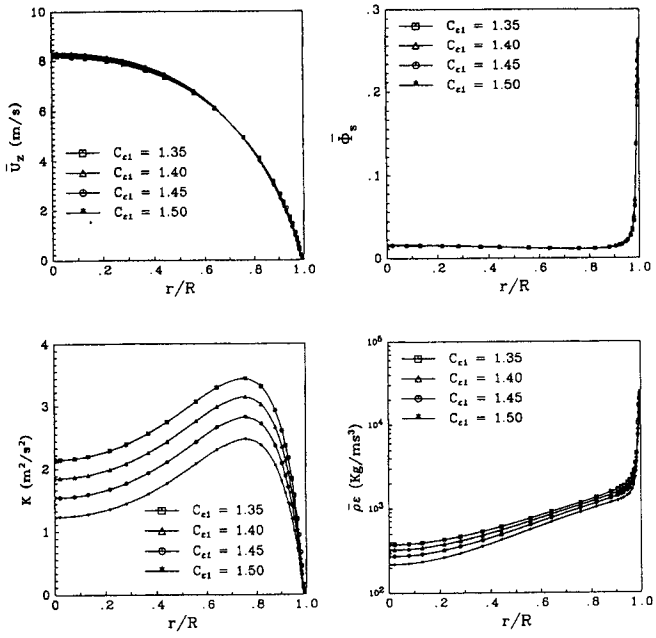

Figure 12. Parametric sensitivity of the model predictions with respect to $C_{\epsilon 1}$.

All other quantities are as in Table 2.

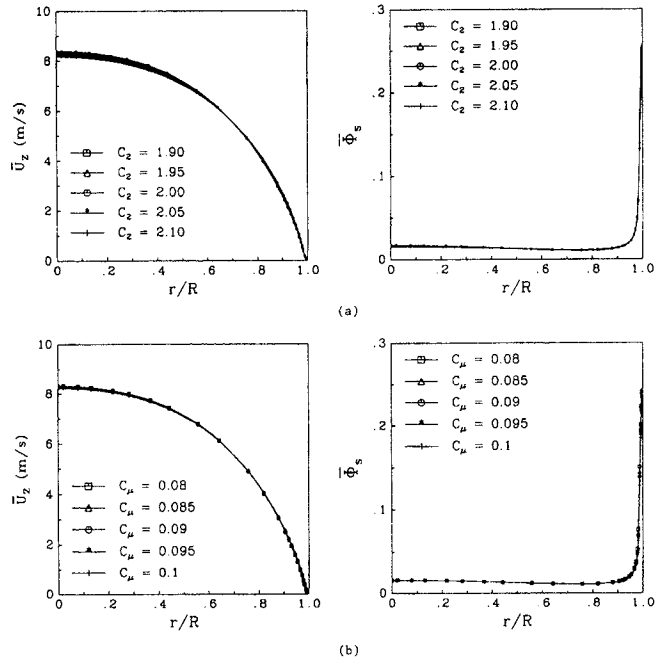

Figure 13. Parametric sensitivity of the model predictions with respect to (a) C_2 and (b) C_μ.

All other quantities are as in Table 2.

and, using this in the above expression:

$$t_g = \frac{1}{18}\frac{(1-\bar{\phi}_s)^n}{\bar{\phi}_s}\frac{d^2\rho_g}{\mu_g}$$

This is used to calculate the curve of t_g shown in Figure 11.

Finally, the dissipation time scale is given by:

$$t_K = (\nu_e/\epsilon)^{1/2}$$

and this determines the third curve in Figure 11.

The scaling assumptions, on which our equations are based, require that both t_g and t_c should be much smaller than t_K, and Figure 11 confirms that this is the case, over the whole cross section.

As noted earlier, the values listed in Table 2 for the constants appearing in the K-ϵ equations are standard for turbulent pipe flow of a homogeneous, incompressible fluid. The use of these same values to generate a model for the turbulence in the particle suspension is highly speculative, so it is important to explore the extent to which our results depend on this choice. Figure 12 shows how $\bar{u}_z$, $\bar{\phi}_s$, K and $\bar{\rho}\epsilon$ are affected by changing $C_{\epsilon 1}$ about the value 1.45 listed in Table 2. The influence on the velocity profile is seen to be small, while the changes in the profile of $\bar{\phi}_s$ are almost imperceptible. The effects on K and $\bar{\rho}\epsilon$ are greater, but these variables have less direct physical importance than $\bar{u}_z$ and $\bar{\phi}_s$. Figures 13a and b show the effects on the velocity and solids fraction profiles of similar variations in the value of C_2, and of variations of approximately 10% in the value of C_μ. The responses are even smaller than in the case of $C_{\epsilon 1}$, and the same is true for the curves of K and $\bar{\rho}\epsilon$, which are not shown here. Finally, Figures 14a and b show the corresponding results for variations of the last pair of parameters, σ_ϵ and σ_K. In this case, the changes in $\bar{u}_z$ and $\bar{\phi}_s$ are scarcely perceptible, while those in K and $\bar{\rho}\epsilon$, not shown, are quite small. It therefore appears that the predictions are fairly insensitive to the values of the constants in the turbulence model. This is a welcome contrast to the sensitivity of the predictions for laminar gas-laminar particles flows (Sinclair and Jackson, 1989; Pita and Sundaresan, 1991; Ocone, Sun-

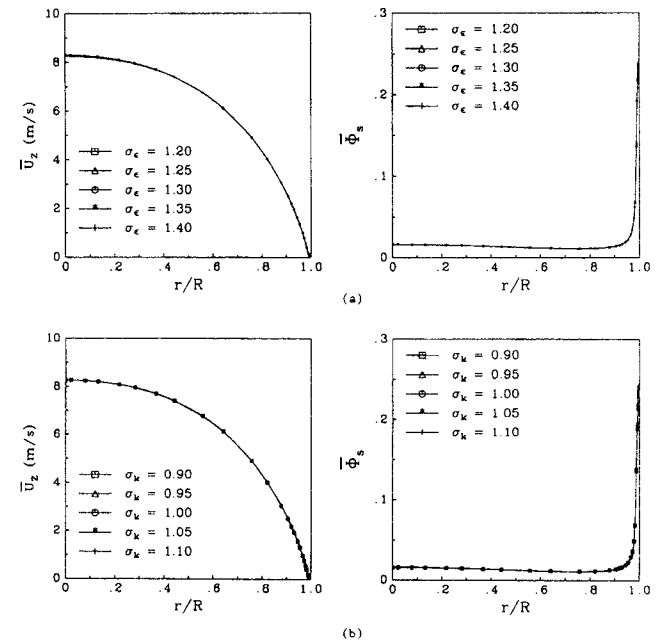

Figure 14. Parametric sensitivity of the model predictions with respect to (a) σ_ϵ and (b) σ_K.

All other quantities are as in Table 2.

daresan and Jackson, 1993), where a very small degree of inelasticity in the collisions between pairs of particles was found to change the results radically.

In the present work, the collective behavior of the particle assembly has been represented by assigning functional forms to the dependence of particle phase pressure, $\bar{p}_s$, and effective viscosity, μ_{es}, on the bulk density $\bar{\rho}$. Thus, the granular temperature, which represents random collision-induced motion of the particles on the scale of λ, has been excluded from the picture. It would not be difficult to reintroduce this, using one of the expressions derived from kinetic theory for the particle phase stress tensor (see, for example, Lun et al., 1984). The equations used here would then have to be supplemented by a differential balance for the pseudothermal energy of this random motion. We intend to explore this in future work.

Finally, we are very conscious of the shortcomings of the crude turbulence closure used here, and intend to explore the direct numerical computation of solutions of the full transient Eqs. 1-5.

Conclusions

Existing work on the turbulent flow of suspensions of solid particles in a gas has been largely confined to the "dusty gas" limit, where the concentration of the particles is very small. The turbulence then has its origin in the instability of laminar flow of the gas, and the presence of the particles serves to modify the properties of the turbulence, when compared with those of a gas flowing without suspended particles.

Here we have considered the opposite limit, where the concentration of particles is high. The particles then interact with each other by collision and this endows the particle assembly with collective properties like those of a gas of very massive molecules, as we now know from recent work on the application of kinetic theory to granular materials. In turbulent pipe flow, we argue that at these concentrations there is a separation in both length and time scales between the turbulence and quantities associated with individual particles and their collisions. Local averaging over a radius intermediate between these scales then yields equations for the motion of the two phases which resemble formally equations for interpenetrating continua. These equations should be applicable in modeling the mean motion and the turbulence.

We then recognize that, at these very high mass loadings, for motions on the scale of the mean flow and the turbulence, both inertial and viscous effects in the suspension are completely dominated by the contributions from the particle phase. Our picture of the generation of turbulent fluctuations is, therefore, quite different from that which applies to the flow of a dilute suspension, or simply a gas. For a dense suspension the gas forced up the pipe by its pressure gradient serves to propel the particles in the same direction, through the drag force exerted on them. Because of the impediment to motion arising from contacts with the pipe walls, the moving assembly of particles is constrained to shear, and it is this shearing of the particle assembly which, through the collective inertia and the effective viscosity arising from collisions between particles, generates the turbulent fluctuations in the particle velocity. The gas then responds to these fluctuations and is the passive participant in the turbulence. Once turbulence is established, there must be a depletion of particles near the axis and a corresponding increase in concentration adjacent to the wall in order to maintain a force balance (including Reynolds stress) in the radial direction. Thus, while the gas pressure gradient is the propelling agent for the flow, and is therefore the ultimate source of energy for the turbulent fluctuations, the role of the gas in generating these fluctuations is an indirect one. In particular, instability of the shear flow of the gas due to the no-slip condition at the pipe wall, which is the origin of turbulence in the flow of gas (or a very dilute suspension), does not play a significant role in the present situation.

Computations for fully developed, turbulent flow in a vertical pipe based on these ideas, though calling for some speculative closures, appear to give a reasonable account of observed behavior.

Acknowledgment

This work has been supported by grants from the International Fine Particle Research Institute and the Mobil Foundation.

Notation

A = solid phase effective pressure factor (Table 2, Eq. 40), $kg \cdot m^{-1} \cdot s^{-2}$
B = solid phase effective viscosity factor (Table 2, Eq. 41), $kg \cdot m^{-1} \cdot s^{-1}$
c = mean velocity of pseudothermal motion of particles, $m \cdot s^{-1}$
C_2, $C_{\epsilon 1}$, C_μ = K-ϵ equation constants given in Table 2
$C_{\epsilon 2}$ = function defined by Eq. 39
d = particle diameter, m
$\underline{\underline{E}}$ = stress tensor for suspension or phase indicated by subscript, $kg \cdot m^{-1} \cdot s^{-2}$
g = specific gravity force, $m \cdot s^{-2}$
g_o = radial distribution function, defined after Eq. 41
$\underline{\underline{I}}$ = identity tensor
K, K_p = turbulent kinetic energy per unit mass of suspension and particles, respectively, $m^2 \cdot s^{-2}$
l_K = dissipation scale, m
n = Richardson-Zaki exponent
p = pressure of suspension or phase indicated by subscript, $kg \cdot m^{-1} \cdot s^{-2}$
r = radial coordinate, m
R = tube radius, m
R_T = turbulent Reynolds number
t = time, s
t_c = collision time scale, s
t_g = gas relaxation time, s
t_K = dissipation time scale, s
$\underline{u}$ = velocity of suspension or phase indicated by subscript, $m \cdot s^{-1}$
$\overline{U}$ = superficial velocity of phase indicated by subscript, $m \cdot s^{-1}$
v_t = terminal velocity of fall of a single particle in a stationary gas, $m \cdot s^{-1}$
z = axial coordinate, m

Greek letters

α = constant
β_1 = drag coefficient, s^{-1}
β = defined as β_1/ϕ_g, s^{-1}
$\tilde{\beta}_1$ = limiting value of β_1 as $\phi_g \to 1$, s^{-1}
ϵ = turbulent dissipation rate per unit mass of suspension, $m^2 \cdot s^{-3}$
θ = angular coordinate, rad
λ = mean separation between particles, m
μ_e = effective viscosity of suspension or phase indicated by a second subscript, $kg \cdot m^{-1} \cdot s^{-1}$
μ_g = viscosity of gas, $kg \cdot m^{-1} \cdot s^{-1}$
ν_e = effective kinematic viscosity, $m^2 \cdot s^{-1}$
ν_T = eddy viscosity defined by Eq. 36, $m^2 \cdot s^{-1}$

ρ = density of suspension or phase indicated by subscript, $kg \cdot m^{-3}$
σ_ϵ, σ_K = parameters in K-ϵ model (Table 2)
ϕ = volume fraction of phase indicated by subscript
ϕ_{sm} = volume fraction of solids at random close packing

Subscripts

g = gas phase
s = solid phase
r, z, θ = component in cylindrical coordinate system

Superscript

$'$ = fluctuation about mean

Literature Cited

Ahmadi, G., and D. Ma, "A Thermodynamical Formulation for Dispersed Multiphase Turbulent Flows: I. Basic Theory & II. Simple Shear Flows for Dense Mixtures," *Int. J. Multiphase Flow*, **16**, 323 (1990).

Anderson, T. B., and R. Jackson, "A Fluid Mechanical Description of Fluidized Beds: Equations of Motion," *Ind. Eng. Chem. Fundam.*, **6**, 527 (1967).

Anderson, T. B., and R. Jackson, "A Fluid Mechanical Description of Fluidized Beds: Comparison with Theory and Experiment," *Ind. Eng. Chem. Fundam.*, **8**, 137 (1969).

Arnason, G., and D. E. Stock, "A New Method to Measure Particle Turbulent Dispersion Using Laser Doppler Anemometer," *Experiments in Fluids*, **2**, 89 (1984).

Bader, R., J. Findlay, and T. M. Knowlton, "Gas/Solid Flow Patterns on a 30.5-cm-Diameter Circulating Fluidized Bed," *Int. Circulating Fluidized-Bed Conf.*, Compiegne, France (Mar. 14-18, 1988).

Bartholomew, R., and R. Casagrande, "Measuring Solids Concentration in Fluidized Systems by Gamma-Ray Absorption," *Ind. Eng. Chem.*, **49**, 428 (1957).

Basu, P., and P. K. Nag, "An Investigation into Heat Transfer in Circulating Fluidized Beds," *Int. J. Heat Mass Transfer*, **30**, 2399 (1987).

Berker, A., and T. Tulig, "Hydrodynamics of Gas-Solids Flow in a Catalytic Cracker Riser: Implications for Reactor Sensitivity Performance," *Chem. Eng. Sci.*, **41**, 821 (1986).

Cebeci, T., and A. M. O. Smith, *Analysis of Turbulent Boundary Layers*, Academic Press, Orlando, FL (1974).

Ding, J., and D. Gidaspow, "A Bubbling Fluidization Model Using Kinetic Theory of Granular Flow," *AIChE J.*, **36**, 523 (1990).

Elghobashi, S. E., and T. W. Abou-Arab, "A Two-Equation Model for Two-Phase Flows," *Phys. Fluids*, **26**, 4 (1983).

Gidaspow, D., Y. P. Tsuo, and K. M. Luo, "Computed and Experimental Cluster Formation in Velocity Profiles in Circulating Fluidized Beds," Int. Fluidization Conf., Banff, Alberta, Canada (May, 1989).

Grace, J. R., "High-Velocity Fluidized Bed Reactors," *Chem. Eng. Sci.*, **45**, 1953 (1990).

Grace, J. R., and J. Tuot, "A Theory for Cluster Formation in Vertically Conveyed Suspensions of Intermediate Density," *Trans. Inst. Chem. Eng.*, **57**(1), 49 (1979).

Hernandez, J. A., and J. Jimenez, "Bubble Formation in Dense Fluidized Beds," *Phys. Fluids A*, **3**, 1457 (1991).

Johnson, P. C., and R. Jackson, "Frictional-Collisional Constitutive Relations for Granular Materials with Application to Plane Shearing," *J. Fluid Mech.*, **176**, 67 (1987).

Johnson, P. C., P. Nott, and R. Jackson, "Frictional-Collisional Equations of Motion for Particulate Flows and Their Application to Chutes," *J. Fluid Mech.*, **210**, 501 (1990).

Lee, S. L., and F. Durst, "On the Motion of Particles in Turbulent Duct Flows," *Int. J. Multiphase Flow*, **8**, 125 (1982).

Louge, M., E. Mastorakos, and J. T. Jenkins, "The Role of Particle Collisions in Pneumatic Transport," *J. Fluid Mech.*, **231**, 345 (1991).

Lumley, J. L., "Two-Plate and Non-Newtonian Flows," in *Topics in Applied Physics*, P. Bradshaw, ed., **12**, 289 (1978).

Lun, C., S. B. Savage, D. Jeffrey, and N. Chepurniy, "Kinetic Theories for Granular Flow: Inelastic Particles in Couette Flow and Slightly Inelastic Particles in a General Flow Field," *J. Fluid Mech.*, **140**, 223 (1984).

Marble, F. E., "Dynamics of Dusty Gases," *Annual Rev. Fluid Mech.*, **2**, 397 (1970).

Matsen, J. M., "Mechanisms of Choking and Entrainment," *Powder Tech.*, **32**, 21 (1982).

Mello, T. M., P. H. Diamond, and H. Levine, "Hydrodynamic Modes of a Granular Shear Flow," *Phys. Fluids A*, **3**, 2067 (1991).

Ocone, R., S. Sundaresan, and R. Jackson, "Gas-Particle Flow in a Duct of Arbitrary Inclination with Particle-Particle Interactions," *AIChE J.*, **39**(8), 1261 (1993).

Patel, V. C., W. Rodi, and G. Scheurer, "Turbulence Models for Near-Wall and Low Reynolds Number Flows: A Review," *AIAA J.*, **23**, 1308 (1985).

Pita, J. A., and S. Sundaresan, "Gas-Solid Flow in Vertical Tubes," *AIChE J.*, **37**(7), 1009 (1991).

Richardson, J., and W. Zaki, "Sedimentation and Fluidization: Part I," *Trans. Instn. Chem. Engrs.*, **32**, 35 (1954).

Rogers, C. B., and J. K. Eaton, "The Effect of Small Particles on Fluid Turbulence in a Flat-Plate, Turbulent Boundary Layer in Air," *Phys. Fluids A*, **3**, 928 (1991).

Rouhiainen, P. O., and J. W. Stachiewicz, "On the Deposition of Small Particles from Turbulent Streams," *J. Heat Transfer*, **92**, 169 (1970).

Saffman, P. Q., "The Lift of a Small Sphere in a Slow Shear Flow," *J. Fluid Mech.*, **22**, 385 (1965).

Savage, S. B., "Instability of Unbounded Uniform Granular Shear Flow," *J. Fluid Mech.*, **241**, 109 (1992).

Saxton, A., and A. Worley, "Modern Catalytic Cracking Design," *Oil and Gas J.*, **68**, 82 (1970).

Schnitzlein, M. G., and H. Weinstein, "Flow Characterization in High-Velocity Fluidized Beds Using Pressure Fluctuations," *Chem. Eng. Sci.*, **43**, 2605 (1988).

Sinclair, J. L., and R. Jackson, "The Effect of Particle-Particle Interactions on the Flow of Gas and Particles in a Vertical Pipe," *AIChE J.*, **35**, 1473 (1989).

Soo, S. L., H. K. Ihrig, and A. F. El Kouh, "Experimental Determination of Statistical Properties of Two-Phase Turbulent Motion," *Trans. ASME D: J. Basic Engrng.*, **82D**, 609 (1960).

Speziale, C. G., "Analytical Methods for the Development of Reynolds Stress Closures in Turbulence," *Annual Rev. Fluid Mech.*, **23**, 107 (1991).

Squires, K. D., and J. K. Eaton, "Particle Response and Turbulence Modification in Isotropic Turbulence," *Phys. Fluids A*, **2**, 1191 (1990).

Tsuji, Y., Y. Morikawa, and H. Shiomi, "LDV Measurements of an Air-Solid Two-Phase Flow in a Vertical Pipe," *J. Fluid Mech.*, **139**, 417 (1984).

Tsuo, Y. P., and D. Gidaspow, "Computation of Flow Patterns in Circulating Fluidized Beds," *AIChE J.*, **36**, 885 (1990).

Weinstein, H., M. Shao, and L. Wasserzug, "Radial Solid Density Variation in a Fast Fluidized Bed," *AIChE Symp. Ser.*, **80**, 117 (1984).

Yerushalmi, J., N. Cankurt, D. Geldart, and B. Liss, "Flow Regimes in Vertical Gas-Solid Contact Systems," *AIChE Symp. Ser.*, **74**, 1 (1978).

Youchou, L., and M. Kwauk, "The Dynamics of Fast Fluidization," *Fluidization*, J. Grace and J. Matsen, eds., Plenum Press, New York (1980).

Manuscript received Feb. 16, 1993, and revision received June 11, 1993.